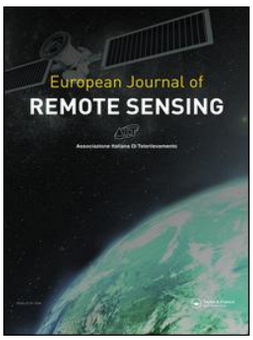

European Journal of Remote Sensing

ISSN: (Print) 2279-7254 (Online) Journal homepage: http://www.tandfonline.com/loi/tejr20

Integration of 3D modeling, aerial LiDAR and photogrammetry to study a synsedimentary structure in the Early Jurassic Calcari Grigi (Southern Alps, Italy)

Marco Franceschi, Mattia Martinelli, Lorenzo Gislimberti, Alessandro Rizzi & Matteo Massironi

To cite this article: Marco Franceschi, Mattia Martinelli, Lorenzo Gislimberti, Alessandro Rizzi & Matteo Massironi (2015) Integration of 3D modeling, aerial LiDAR and photogrammetry to study a synsedimentary structure in the Early Jurassic Calcari Grigi (Southern Alps, Italy), European Journal of Remote Sensing, 48:1, 527-539, DOI: 10.5721/EuJRS20154830

To link to this article: http://dx.doi.org/10.5721/EuJRS20154830

Published online: 17 Feb 2017.

European Journal of Remote Sensing - 2015, 48: 527-539
doi: 10.5721/EuJRS20154830
Received 06/11/2014, accepted 19/02/2015

European Journal of Remote Sensing
An official journal of the Italian Society of Remote Sensing

www.aitjournal.com

Integration of 3D modeling, aerial LiDAR and photogrammetry to study a synsedimentary structure in the Early Jurassic Calcari Grigi (Southern Alps, Italy)

Marco Franceschi[1]*, Mattia Martinelli[1], Lorenzo Gislimberti[1], Alessandro Rizzi[2] and Matteo Massironi[1]

[1]Department of Geosciences, Università degli Studi di Padova, via Gradenigo, 6, 35131, Padova, Italy
[2]SMART3K S.R.L., via Sommarive, 18, 38123, Trento, Italy
*Corresponding author, e-mail address: marco.franceschi79@gmail.com

Abstract

LiDAR and photogrammetry data are integrated to study an Early Jurassic extensional synsedimentary structure in the Italian Southern Alps. Airborne LiDAR data helped in getting geologic information in areas covered by vegetation, photogrammetry was applied to produce a high-resolution 3D textured model of the inaccessible parts of the outcrop. LiDAR and photgrammetric data were merged together producing a multi-resolution model. Key geologic boundaries and faults bounding the synsedimentary structure were digitized in a 3D geomodeling environment. The reconstruction yielded information about the structure kinematics and accumulated displacements.

Keywords: 3D modeling, photogrammetry, LiDAR, synsedimentary tectonics, Early Jurassic.

Introduction

The integration of geologic 3D modeling and remote sensing techniques has become a diffused practice in the study of outcrops [McCaffrey et al., 2005; Trinks et al., 2005]. Petroleum industry has been the major driver of the advances in these approaches. The reason for this lies in the capability of outcrop modelling of filling the gap in scale range between geophysical investigations and log observations and, hence, helping in capturing the potential reservoir heterogeneities [Jones et al., 2008]. Remote sensing techniques have two primary strengths: 1) they allow studying outcrops that for their exposition and/or size could not otherwise be easily examined with traditional methods; 2) allow a quantitative approach which results extremely useful for modeling purposes. Both active, e.g. laser scanning [Hodgetts, 2013], and passive, e.g. hyperspectral imaging and photogrammetry [Buckley et al., 2013; Tavani et al., 2014], have been successfully applied to outcrop modeling. Among the laser scanning devices, airborne Light Detection And Range (LiDAR) systems are used to produce digital elevation models of the topographic surface and to

highlight morphological features even beneath the vegetation canopy. Photogrammetry is a technique that permits to produce 3D models of objects starting from 2D images acquired with a camera. The portability of camera systems, which far exceeds that of laser scanners, make this technique very flexible in many operational contexts. Successful examples of application of photogrammetry to structural outcrop modeling are found, for instance, in Bistacchi et al., [2011], Assali et al. [2014] and Martín et al. [2013].

In this paper we present an example of integration of photogrammetry and airborne LiDAR to study an outcrop where a synsedimentary extensional structure is exposed (mount Cornello, Southern Alps, Italy). The exposure's conditions, a virtually inaccessible vertical wall, have so far discouraged a detailed characterization of the structure, which was previously described by Doglioni and Bosellini [1987] and Avanzini et al. [2012] on the basis on 2D images and drawings. The application of geologic 3D modeling techniques has allowed representing the mount Cornello structure in his three dimensionality for the first time. This allowed a more quantitative reconstruction of the faulting geometry and the estimate of the displacements across each fault.

To the best of our knowledge, this represents the first example of application of this integrated approach to the investigation of outcropping synsedimentary structures in extensional geodynamic contexts. Usually 3D models of extensional structures are reconstructed starting from seismic data [Beidinger and Decker, 2011] or through sandbox modeling [Wu et al., 2009]. Few studies have been dedicated to the study of outcropping examples and yet no digital model has been realized starting from outcrop data of extensional synsedimentary structures. In this work we show how the integration of LiDAR data, photogrammetry, 3D geomodeling and classical geologic mapping is a readily applicable method for structural analysis where exposure conditions prevent direct access.

Geological Setting

The Early Jurassic was a period of important continental reorganization that brought to the Pangea mega-continent break-up [Smith et al., 1994]. In the area now occupied by the Italian Southern Alps, rifting caused the formation of a series of structural highs characterized by shallow water carbonate precipitation and lows where deep-water sediments deposited [Winterer and Bosellini, 1981]. The Calcari Grigi Group [Avanzini et al., 2006] encompasses the Early Jurassic sediments deposited on one of these highs.

Rifting-induced synsedimentary tectonics in the area [Bertotti, 2001; Berra and Carminati, 2010] is testified by the presence of synsedimentary faults and structures and by sharp and abrupt thickness-variations in the Calcari Grigi Group's stratigraphic units [Masetti et al., 1998, 2012; Franceschi et al., 2014a].

The study area is located close to Mezzolombardo village (Fig. 1A) and is covered by the 1:50000 "Mezzolombardo"geological map [Avanzini et al., 2012]. The present structural setting is dominated by a series of approximately N/S and NE/SW trending faults and thrusts. To the W of the study area the main structural feature is the Trento-Cles line, interpreted as a Mesozoic extensional fault reactivated with a strike slip kinematics during the Neogene [Prosser, 1998; Massironi et al., 2006]. To the East, there are the alpine Mezzolombardo-Taio fault, interpreted as left-lateral strike slip fault, and the Paganella thrust system (Fig. 1A).

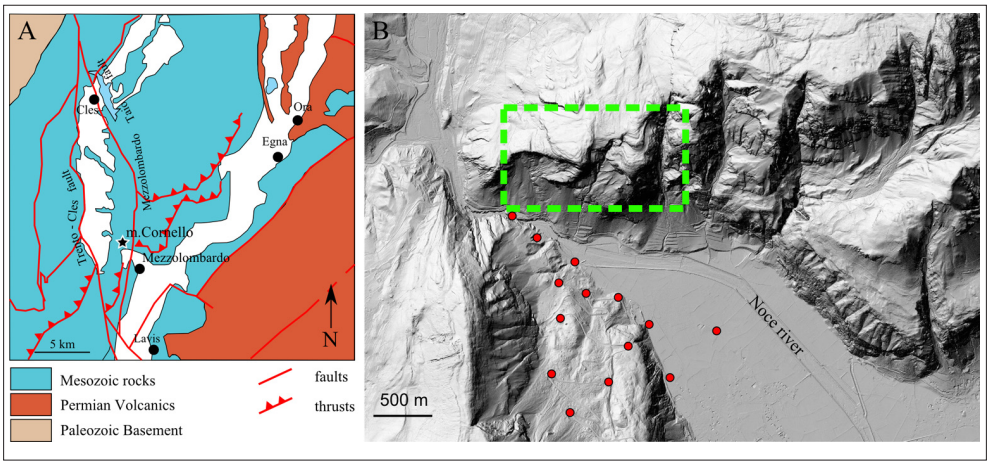

Figure 1 - A) Simplified geologic map (from Avanzini et al. [2012], modified) with major faults indicated. Position of M. Cornello is highlighted (star). B) View points (dots) of the high-resolution images taken for the realization of the photogrammetric model of the M. Cornello structure. Location of the structure is highlighted by a green dashed square.

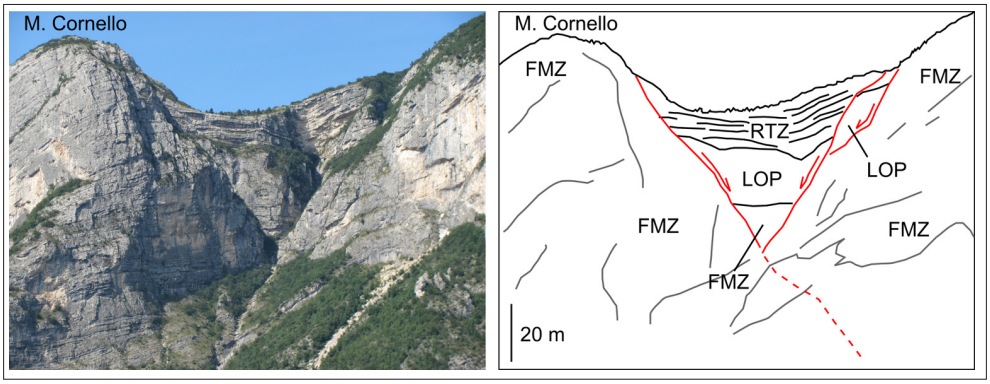

Figure 2 - Left. mount Cornello (46°14′13.53″N, 11°04′42.22″E). Right: line drawing highlighting the Early Jurassic negative flower structure. RTZ = Rotzo Formation; LOP = Loppio Oolitic Limestone Formation; FMZ = Monte Zugna Formation.

The structure object of this study is spectacularly exposed on the southern slope of mount Cornello (46°14′13.53″N, 11°04′42.22″E) in the Trentino Province (Italy) (Fig. 2). The stratigraphic succession at mount Cornello is the following, from bottom to top: (a) Monte Zugna Formation (Hettangian-Sinemurian), (b) Loppio Oolitc Limestone (Sinemurian p.p.) and (c) Rotzo Formation (Pliensbachian p.p.) [Masetti et al., 1998 for a detailed description of the depositional environments]. The current structural setting of mount Cornello is related to Alpine compression along and consists of a broad anticline with a ENE/WSW-trending NNW/SSE-dipping axial plane. Beds attitude is to NNW. The mount Cornello structure consists of a series of approximately N/S-trending synsedimentary faults cross-cutting the Early Jurassic formations (Fig. 2B) [Doglioni and Bosellini,1987; Avanzini et al., 2012].

Doglioni and Bosellini [1987] did not subdivide the Calcari Grigi Group into different formations, hence they were not able to distinguish multiple deformation phases within the Early Jurassic activity of the synsedimentary normal faults. By contrast, Avanzini et al. [2012] provided a finer stratigraphic framework that allowed two extensional phases of deformation to be recognized. In the first phase, Sinemurian in age, one of the faults was active during the deposition of the Monte Zugna formation as testified by its thickness variations. A stasis in the differential subsidence is testified by the rather constant thickness of the Loppio Oolitic Limestone. A second extensional pulse was Pliensbachian in age and is responsible of the activation of the synsedimentary faults that dissect the Loppio Oolitic Limestone, displacing it and again inducing differential subsidence testified by thickness variations the Rotzo formation.

Material and Methods

The study area is covered by a 1 m resolution DTM obtained from aerial acquisitions realized by the Provincia Autonoma di Trento. LiDAR data were used to produce a first-order 3D model of the topographic surface of the mount Cornello area. This was useful as reference framework for the field observations and helped in producing the geologic map.
Aerial LiDAR gives a good description of flat to low-inclined surfaces, even in vegetated areas, but steep or vertical areas are poorly resolved because the acquisition is carried out with a nadir-looking device. Since the mount Cornello structure is best exposed on the southern vertical slope of the mountain, LiDAR did not help in investigating that area. Photogrammetry was instead applied to reconstruct the outcrop's vertical walls in 3D and get relevant geometric information on the synsedimentary structure.
Photogrammetry allows the 3D reconstruction of an object's surface starting from a set of 2D overlapping photographs taken from different view-points, provided that the intrinsic parameters of the camera and the acquisition geometry are known [Remondino and El-Hakim, 2006]. Crucial steps in this process are the image-network planning to achieve complete coverage of the target and the calculation of the image orientation to perform bundle adjustment [Baltsavias et al., 2008]. A D3X Nikon camera with a 135 mm Nikkor lens was used to acquire 16 high-resolution images in a frontal position with respect to the target at an approximate distance of 4 km (Fig. 1B). This allowed a ground-sample-distance (GSD) between 0.05 m and 0.1 m. To cover the portions of the target that were not visible from the frontal acquisitions, 62 images were acquired using a Nikon D800E camera equipped with 50 mm Nikkor lens. In this case the acquisition were performed from sites located in the close surroundings of the mount Cornello structure at a distance ranging from 50 m to 300 m.
All the view-points were georeferenced with GPS (Geotagger Pro 2 - Solmeta) connected to the cameras. Image processing was carried out with Agisoft Photoscan® to obtain a scaled and georeferenced 3D model. Six overlapping point-clouds (average resolution 0.25 m) with RGB values associated to each point were merged together to create a complete 3D model.
LiDAR and photogrammetric models were merged using Geomagic Studio® producing a multi-resolution 3D model. Alignment was obtained on the basis of the georeferencing and refined applying Iterative Closest Point (ICP) algorithm [Besl and McKay, 1992]. Since models were obtained with different methods and had different resolution, perfect

alignment was not possible and the final standard deviation registration error resulted 0.43 m between the six photogrammetric models and 1.8 m between photogrammetric and LiDAR (DEM) models.

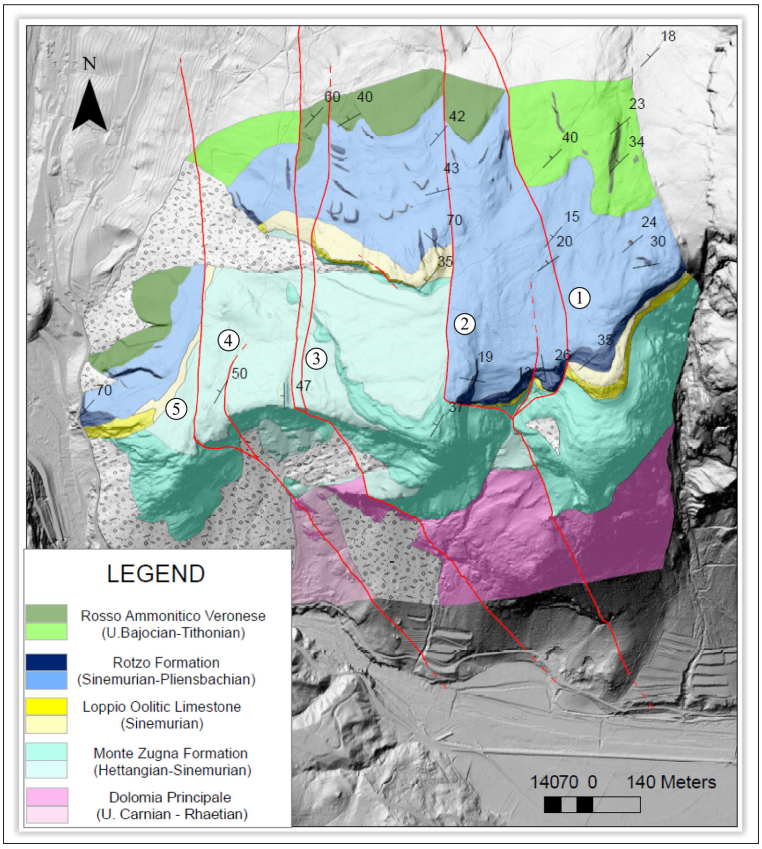

Figure 3 - Geologic map of the study area. Darker color marks outcrops, lighter color interpreted areas. Main faults are numbered from 1 to 5.

Geologic mapping of the study area was undertaken at 1:10000 scale to produce a new digital geologic map in GIS environment (Fig. 3). As criteria for distinguishing the stratigraphic units of the Calcari Grigi Group, we used those adopted for the Mezzolombardo sheet [Avanzini et al., 2012]. Being beyond the scopes of this contribution, we do not report a complete description of the Calcari Grigi units and of their distinctive features, however detailed informations can be found in Masetti et al. [1998] and Avanzini et al. [2012]. LiDAR DTM obtained considering last-pulse laser signal were helpful in tracing faults and geologic boundaries in the areas covered by the vegetation. Field observations were carried out with the help of differential GPS.

The 3D point cloud derived from the complete multi-resolution model was imported in SKUA® geomodeling software as 3D data in the form x, y, z, i. The i parameter carried the photographic greyscale texture information of each point. Imported points were then transformed into a triangular 3D mesh.

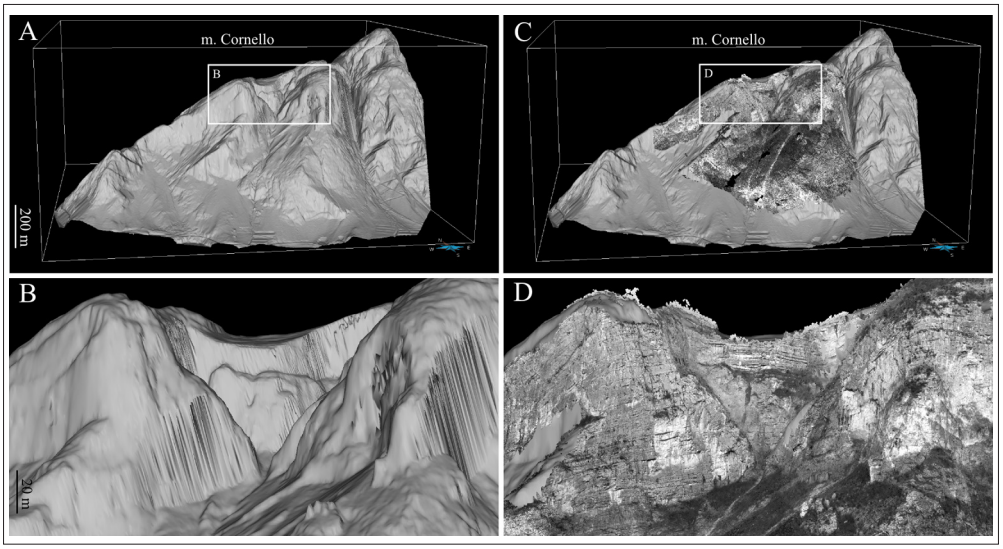

Figure 4 - A) LiDAR-derived 3D model of the study area. Note (B) the low-resolution of the vertical cliffs. C) Multiresolution 3D model obtained from the integration of LiDAR and photogrammetry data. D) Detail showing the improvement in resolution in the vertical areas.

Figure 4A and 4B shows the LiDAR derived model before the integration of the photogrammetric model while Figure 4C and 4D shows the same view of the integrated model and highlight the sensible improvement in terms of resolution on the vertical cliffs.
The multi-resolution 3D model of the mount Cornello's surface allowed us to directly digitize the boundaries of the outcropping geologic units and the faults. Hence, the digitized polylines were used to improve the accuracy of the geologic map. Geologic cross sections were drawn starting from the 3D-model-corrected geologic map.
The geological cross sections were built using the specific tool embedded in SKUA® that permit to easily get a topographic profile and digitize the geologic interpretation. In particular, four digitized geologic cross sections, including all the intercepted geologic boundaries and faults, were drawn on the basis of the geologic map and displaying. In SKUA® the cross sections are shown as vertical 3D planes in their exact position (Fig. 6). This permits to easily cross-check the geologic interpretation with the geologic map and the cross cutting sections. The polylines digitized on the geologic map, on the 3D surface model and on the cross sections together with available layers and faults attitude measurements were used as constraints to model the 3D surfaces of unit boundaries and faults in SKUA® working in its Structure&Stratigraphy module.

Results

The geologic map of the area is shown in Figure 3. The map essentially agrees with the "Mezzolombardo" 1:50000 sheet, but the finer scale allowed a better mapping of Loppio Oolitic Limestone in the study area. This was important in the 3D modeling phase to characterize the upper part of the mount Cornello structure, which essentially influenced the deposition of the Rotzo formation, and to calculate the synsedimentary tectonics-induced

thickness variations.
The final model of the structure and the geologic map show a series of NNW/SSE trending conjugate faults.
The structure (Fig. 5 A-B), is formed by a series of NNW/SSE-trending, ENE-dipping normal faults (2, 3, 4, 5) and a conjugate NNW/SSE-trending, WSW-dipping normal fault (1).
Original dip-angles of the faults, prior to Alpine uplift, range from 50° to 70° which are the cut off angles between the bedding and the fault surfaces.

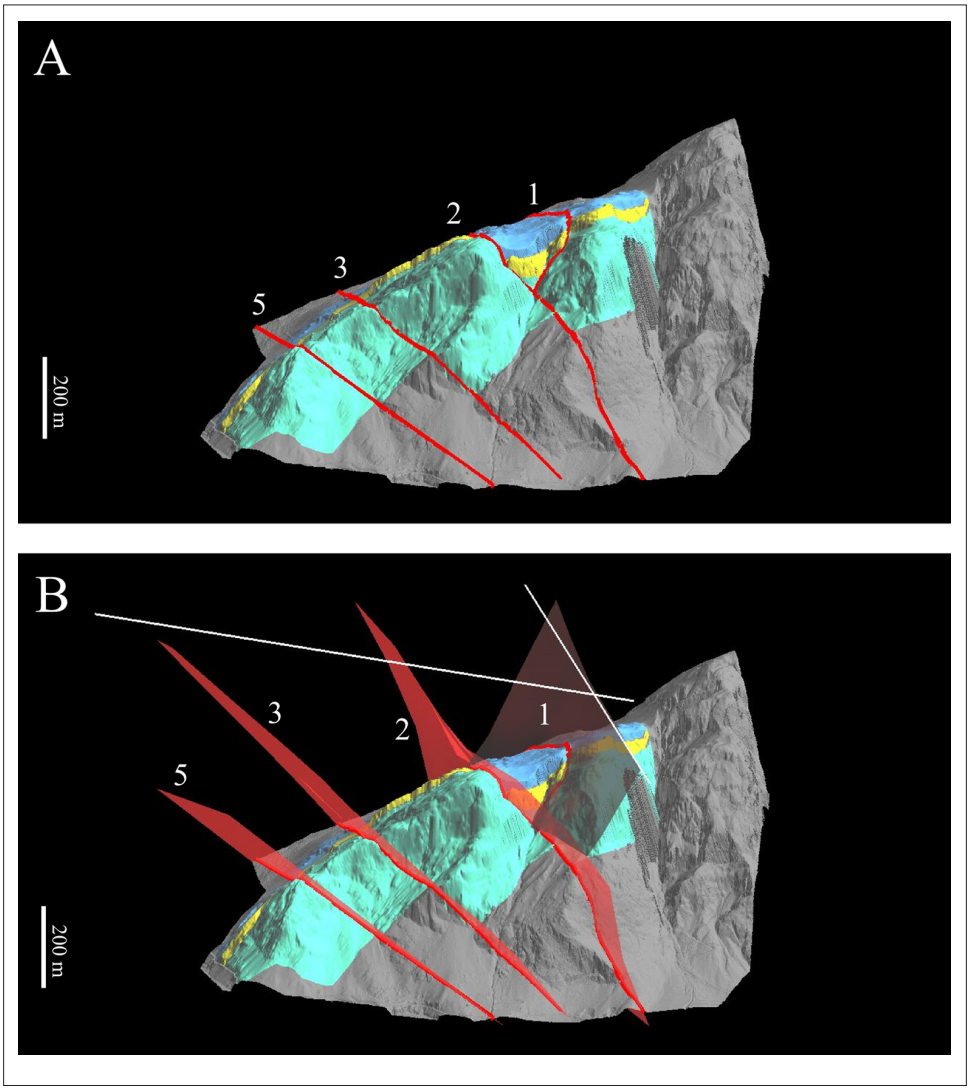

Figure 5 - A) SKUA® 3D geologic model of the mount Cornello structure with Monte Zugna formation, Loppio Oolitic Limestone and Rotzo formation highlighted. Faults labels and colors of the displayed geologic units are the same of Figure 3. B) faults displayed in 3D and traces of cross-sections (white lines) highlighted.

The geologic cross sections (e.g., Fig. 6) and the 3D model highlight a considerable increase in thickness of the Monte Zugna formation from E (370 m) to W (560 m). The maximum thickness is reached close to fault (3). Across fault (3), westward, the Monte Zugna formation is 450 m thick. This is what it retrieved from the 3D reconstruction of the boundary between the Monte Zugna formation and the underling Dolomia Principale as it is traced in the Mezzolombardo map. However, it is important to underline that the lower boundary of Monte Zugna formation is often difficult to locate due to a dolomitization belt of variable thickness at its base; hence, any thickness estimate of the Monte Zugna formation should be taken with caution.

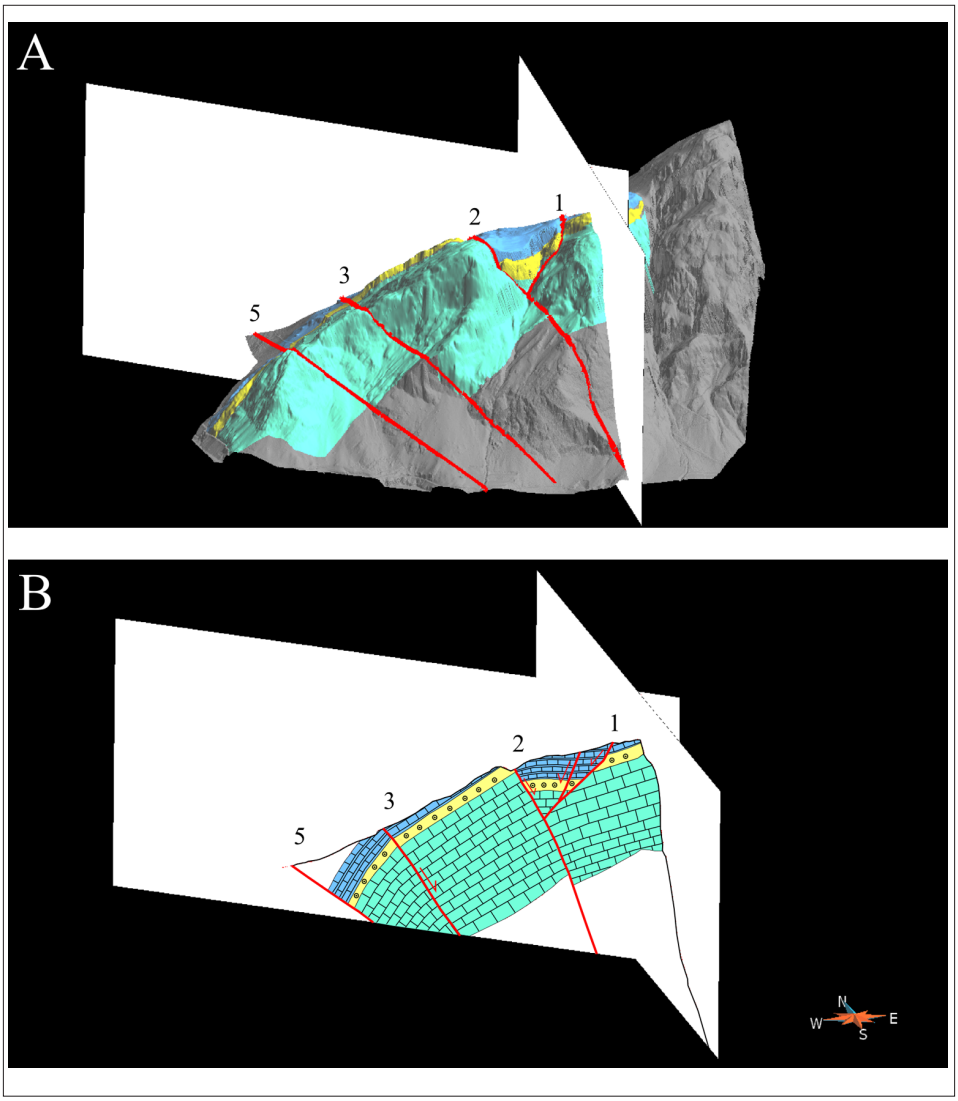

Figure 6 - A) 3D planes of cross sections shown in Figure 5A. B) Cross sections realized on from the 3D model of the mount Cornello structure. Fault labels and colors of geologic units are the same of Figure 3.

Instead, thicknesses of the Rotzo formation can be assessed with higher accuracy because of the sharp contact with the Loppio Oolitic limestone (lower boundary) and the overlying Rosso Ammonitico Veronese (upper boundary) (see Fig. 4). Between the W-dipping fault (1) and the E-dipping fault (2) the Rotzo formation is 240 m-thick, while outside the area bounded by the two faults thickness is 90 m to the W and 130 m to the E. The Rotzo formation thickness further decrease westward reaching only 35 m. at the Rocchetta section, located few kilometers to the W of the study area [Franceschi et al., 2014b]. The Loppio Oolitic Limestone does not display significant thickness variation. Thickness variations across the faults unequivocally testify for the synsedimentary extensional nature of the mount Cornello structure.

The visible variations in thickness of the Rotzo formation and Monte Zugna formation allowed estimating the dip-slip displacement of the faults. The most significant with this respect are fault (2) and (3) (Fig. 4) that trend NNW/SSE and dip approximately 60° to the WSW. Across fault (3) a difference in thickness is visible both in the Monte Zugna formation (110 m) and in the Rotzo formation (20 m), the cumulative dip-slip displacement can be estimated in approximately 160 m. Across fault (2) the difference in thickness in the Rotzo formation is approximately 100 m, hence the dip-slip displacement is 130 m.

Transcurrent Alpine reactivation of the fault system is evidenced by the presence of kinematic indicators on fault planes and by the right lateral offset of Rotzo-Rosso Ammonitico geological boundary. A dextral strike-slip kinematic along NNW-SSE faults is kinematically consistent with the nearby sinistral N/S-trending Mezzolombardo-Taio and Trento-Cles faults (Fig. 1A), being the overall Alpine maximum compressional axis in-between these two orientations.

Discussion and Conclusions

In this study, we have characterized an ancient exhumed extensional tectonic structure by integrating remote sensing, 3D modelling and geologic mapping.

Aearial LIDAR highlighted geologic boundaries and fault traces even in areas covered by the vegetation canopy. Photogrammery allowed the high-resolution 3D imaging of the portion of structure exposed on the inaccessible vertical parts of the studied outcrop. The choice of photogrammetry instead of terrestrial laser scanning was driven by practical considerations since the complexity of the outcrop required several viewpoints, some of which on the outcrop itself, to be described completely.

Altogether, the acquired data permitted to highlight and digitize in 3D key-geologic features (faults and stratigraphic boundaries) with an accuracy otherwise not possible.

The integration of the photogrammetric model with available LiDAR of the study area yielded a complete 3D multi-resolution model of the structures. This was useful in improving the accuracy of the GIS-based geologic map of the area.

3D geomodeling (SKUA®) was used to reconstruct fault planes and stratigraphic boundaries in three dimensions. The 3D geo-model allowed to precisely and easily determine the faults' strikes and dips. It also helped to calibrate the cross sections and to determine the thickness variations in the lithostratigraphic units interested by the structure. This brought unequivocal evidence of the synsedimentary activity of the faults.

The mount Cornello structure can be divided into a lower and an upper part. The lower part displays changes in thickness in Monte Zugna Formation, in particular close to fault

(3). This was interpreted as a growth structure by Doglioni and Bosellini [1987] The upper part mainly interests the Rotzo formation, which shows a significant increase in thickness in particular between fault (1) and (2). The Loppio Oolitic Limestone in between Monte Zugna Formation and Rotzo formation do not show any thickness variation and appear to be passively dissected by the faults. The upper part of the structure, with the clear involvement of the Rotzo formation, was not characterized by Doglioni and Bosellini [1987] because they did not adopted the internal subdivision of the Calcari Grigi Group, but is described in the notes of the "Mezzolombardo" 1:50000 sheet [Avanzini et al., 2012]. However, there seems to be a discrepancy between the synsedimentary faults drawn on the "Mezzolombardo" geologic map and the line drawing presented on the interpreted pictures within the notes. In the geologic map faults (2) and (3) are sharp and parallel whereas in the line drawing fault (3) is listric abruptly changing its dip into a pellicular flat surface at the base of the Loppio Limestones. The interpretation of the 3D model realized in this study favors the interpretation proposed in the geologic map even though the trajectory of fault (2) is now slightly revised.

Thickness variations in the Monte Zugna and the Rotzo formations obtained from the 3D model confirm the interpretation of Avanzini et al. [2012] and testify at least two pulses of activity. One Sinemurian that was responsible for a differential subsidence during Monte Zugna deposition and one Pliensbachian that caused thickness variations in the Rotzo Formation and passively displaced the Loppio Ooltic Limestone.

The 3D model allowed also estimating the dip-slip displacement across the major faults of the mount Cornello structure. In particular fault (3), displaying a synsedimentary activity during the deposition of both the Rotzo and the Monte Zugna formations, has a cumulative offset of 160 m, whereas fault (2) induces thickness variations only in the Rotzo formation with a dip-slip displacement of 120. According to the displacement-length scaling relationships for normal faults [Kim and Sanderson, 2005; Torabi and Berg, 2011], this value suggest a length of these extensional faults in the order of the tens of kilometers at the time of its Mesozoic activity.

Although slightly reactivated during the Alpine deformation, the attitudes and kinematics of the faults still preserve the traces of their ancient activity and are consistent with an E-W regional extension associated with the Early Jurassic rifting in the area [Bertotti, 2001].

Acknowledgements

Authors thank the Servizio Geologico della Provincia Autonoma di Trento and the MUSE-Museo delle Scienze. Dr. Fabio Remondino and the 3DOM unit (FBK - Trento) and Stefano Castelli (Univeristy of Padova) provided technical support in the photogrammetric modelling. Marco Franceschi was funded in the frame of the GEO3DMAP project, part of the "Trentino" project (postdoc - Incoming 2010) Marie Curie Actions - COFUND of the EU FP7 'People' Program.

References

Assali P., Grussenmeyer P., Villemin T., Pollet N., Viguier F. (2014) - *Surveying and modeling of rock discontinuities by terrestrial laser scanning and photogrammetry: semi-automatic approaches for linear outcrop inspection*. Journal of Structural Geology, 66: 102-114. doi: http://dx.doi.org/10.1016/j.jsg.2014.05.014.

Avanzini M., Bargossi G.M., Borsato A., Cucato M., Morelli C., Picotti V., Selli L. (2012) - *Note illustrative della Carta Geologica d'Italia alla scala 1:50.000. Foglio 043 Mezzolombardo*. ISPRA - Servizio Geologico d'Italia.

Avanzini M., Masetti D., Romano R., Podda F., Ponton M. (2006) - *Calcari Grigi*. In: Catalogo delle Formazioni - Unità Tradizionali, Cita M.B., Abbate E., Balini M., Conti M.A., Farloni P., Germani D., Groppelli G., Manetti P., Petti F.M. (Eds.). Carta Geologica d'Italia 1:50000 - Quaderni Serie III, 7 (7): 125-135.

Baltsavias E., Gruen A., Eisenbeiss L., Zhang L., Waser L.T. (2008) - *High-quality image matching and automated generation of 3D models*. International Journal of Remote Sensing, 29 (5): 1243-1259. doi: http://dx.doi.org/10.1080/01431160701736513.

Berra F., Carminati E. (2010) - *Subsidence history from backstripping analysis of the Permo-Mesozoic succession of the Central Southern Alps (Northern Italy)*. Basin Research, 22: 952-975.

Bertotti G. (2001) - *Subsidence, deformation, thermal and mechanical evolution of the Mesozoic South-Alpine rifted margin: an analog for Atlantic-type margins*. In: Non-volcanic rifting of continental margins: a comparison of evidence from land and sea. Wilson R.C.L., Whitmarsh R.B., Taylor B., Froitzheim N. (Eds.). Geological Society, London, 187: 125-141. doi: http://dx.doi.org/10.1144/GSL.SP.2001.187.01.07.

Beidinger A., Decker K. (2011) - *3D geometry and kinematics of the Lassee flower structure: implications for segmentation and seismotectonics of the Vienna Basin strike-slip fault, Austria*. Tectonophysics, 499: 22-40. doi: http://dx.doi.org/10.1016/j.tecto.2010.11.006.

Besl P.J., McKay N.D. (1992) - *A method for registration of 3-d shapes*. IEEE Transactions on Pattern Analysis and Machine Intelligence, 14 (2): 239-256. doi: http://dx.doi.org/10.1109/34.121791.

Bistacchi A., Griffith W.A., Smith S.A.F., Di Toro G., Jones R., Nielsen S. (2011) - *Fault Roughness at Seismogenic Depths from LIDAR and Photogrammetric Analysis*. Pure and Applied Geophysics, 168: 2345-2363. doi: http://dx.doi.org/10.1007/s00024-011-0301-7.

Buckley S.J., Kurz T.H., Howell J.A., Schneider D. (2013) - *Terrestrial lidar and hyperspectral data fusion for geological outcrop analysis.* Computer & Geosciences, 54: 249-258. doi: http://dx.doi.org/10.1016/j.cageo.2013.01.018.

Doglioni C., Bosellini A. (1987) - *Eoalpine and mesoalpine tectonics in the Southern Alps*. Geologische Rundschau, 76: 735-754. doi: http://dx.doi.org/10.1007/BF01821061.

Franceschi M., Massironi M., Franceschi P., Picotti V. (2014a) - *Spatial analysis of thickness variability applied to an Early Jurassic Carbonate Platform in the central Southern Alps (Italy): a tool to unravel synsedimentary faulting*. Terra Nova, 26: 239-246. doi: http://dx.doi.org/10.1111/ter.12092.

Franceschi M., Dal Corso J., Posenato R., Roghi G., Masetti D., Jenkyns H.C. (2014b) - *Early Pliensbachian (Early Jurassic) C-isotope perturbation and the diffusion of the Lithiotis Fauna: Insights from the western Tethys.* Palaeogeography, Palaeoclimatology, Palaeoecology, 410: 255-263. http://dx.doi.org/10.1016/j.palaeo.2014.05.025.

Hodgetts D. (2013) - *Laser scanning and digital outcrop geology in the petroleum industry: a review*. Marine and Petroleum Geology, 46: 335-354. doi: http://dx.doi.org/10.1016/j.marpetgeo.2013.02.014.

Jones R.R., McCaffrey K.J.W., Imber J., Whightman R., Smith S.A.F., Holdsworth R.E., Clegg P., De Paola N., Healy D., Wilson R.W. (2008) - *Calibration and validation of reservoirs models: the importance of high resolution, quantitative outcrop analogues*. In: Robinson A., Griffiths P., Price S., Hegre J., Muggeridge A. (Eds), The Future of Geological Modeling in Hydrocarbon Development, The Geological Society, London, 309: 87-98. doi: http://dx.doi.org/10.1144/SP309.7.

Kim Y.S., Sanderson D.J. (2005) - *The relationship between displacement and length of faults: a review*. Earth-Science Reviews, 68: 317-334. doi: http://dx.doi.org/10.1016/j.earscirev.2004.06.003.

Martín S., Uzkeda H., Poblet J., Bulnes M., Rubio R. (2012) - *Construction of accurate geological cross-sections along trenches, cliffs and mountain slopes using photogrammetry*. Computer & Geosciences, 51: 90-100. doi: http://dx.doi.org/10.1016/j.cageo.2012.09.014.

Masetti D., Claps M., Giacometti A., Lodi P., Pignatti P. (1998) - *The Calcari Grigi Formation of the Trento Platform (Early and Middle Lias, Venetian Prealps)*. Atti Ticinensi di Scienze della Terra, 40: 139-183. doi: http://dx.doi.org/10.1306/03091211087.

Masetti D., Fantoni R., Romano R., Sartorio D., Trevisani E. (2012) - *Tectonostratigraphic evolution of the Jurassic extensional basins of the eastern and southern Alps and Adriatic foreland based on an integrated study of surface and subsurface data*. American Association of Petroleum Geologists Bulletin, 96 (11): 2065-2089.

Massironi M., Zampieri D., Caporali A. (2006) - *Miocene to present major fault linkages through the Adriatic indenter and the Austroalpine-Penninic collisional wedge (Alps of NE Italy)*. Geological Society, 262: 245-258. doi: http://dx.doi.org/10.1144/GSL.SP.2006.262.01.15.

McCaffrey K.J.W., Jones R.R., Holdsworth R.E., Wilson R.W., Clegg P., Imber J., Holliman N., Trinks I. (2005) - *Unlocking the spatial dimension: Digital technologies and the future of geoscience fieldwork*. Journal of the Geological Society, 162 (6): 927-938. doi: http://dx.doi.org/10.1144/0016-764905-017.

Prosser G. (1998) - *Strike-slip movements and thrusting along a transpressive fault zone: the North Giudicarie line (Insubric line, northern Italy)*. Tectonics, 17: 921-937. doi: http://dx.doi.org/10.1029/1998TC900010.

Remondino F., El-Hakim S. (2006) - *Image-based 3D modelling: a review*. The Photogrammetric Record, 21 (115): 269-291. doi: http://dx.doi.org/10.1111/j.1477-9730.2006.00383.x.

Smith A.G., Smith D.G., Funnel B.M. (1994) - *Atlas of Mesozoic and Cenozoic Coastlines*. Cambridge University Press, 99 pp.

Tavani S., Granado P., Corradetti A., Girundo M., Iannace A., Arbués P., Muñoz J.A., Mazzoli S. (2014) - *Building a virtual outcrop, extracting geological information from it, and sharing the results in Google Earth via OpenPlot and Photoscan: an example from the Khaviz Anticline (Iran)*. Computer & Geosciences, 63: 44-53. doi: http://dx.doi.org/10.1016/j.cageo.2013.10.013.

Torabi A., Berg S.S. (2011) - *Scaling of fault attributes: a review*. Marine and Petroleum Geology, 28: 1444-1460. doi: http://dx.doi.org/10.1016/j.marpetgeo.2011.04.003.

Trinks I., Clegg P., McCaffrey K.J.W., Jones R., Hobbs R., Holdsworth B., Holliman N., Imbe J., Waggott S., Wilson R. (2005) - M*apping and analysing virtual outcrops.* Visual

Geosciences, 10 (1): 13-19. doi: http://dx.doi.org/10.1007/s10069-005-0026-9.
Winterer E.L., Bosellini A. (1981) - *Subsidence and Sedimentation on a Jurassic Passive Continental Margin, Southern Alps, Italy*. American Association of Petroleum Geologists Bulletin, 65 (3): 394-421.
Wu J., McCla K., Whitehouse P., Dooley T. (2009) - *4D analogue modelling of transtensional pull-apart basins*. Marine and Petroleum Geology, 26: 1068-1623.